SUPPORTING INFORMATION

Supplemental Table 1: Primers used in PurE Mutagenesis

Primer ID	Primer Name	Sequence (5'→3')[a]
1	H45N.KUNK	CGGGGGTGCG**GTT**AGCAGAAACCAC
2	H45Q.KUNK	TATCGGGGGTGCG**TTG**AGCAGAAACC
3	H45W.DN	GGGGGTGCG**CCA**AGCAGAAACCACTTCAACGTG

[a]Mutagenic sites are in bold.

Supplemental Table 2: $\Delta\varepsilon_{250}$ and Rates of CAIR Decarboxylation at Various pH Values

pH	$\Delta\varepsilon_{250}$ (M^{-1} cm^{-1})	Non-enzymatic CAIR Decomposition (ΔA_{250}/min)
5.1	2129	-0.02
5.6	3650	-0.01
6.1	4646	-0.01
6.6	5331	-0.01
7.0	5513	0.00
7.3	5955	0.00
7.6	6083	0.00
7.9	6230	0.00
8.2	6091	0.00
8.5	5970	0.00
8.8	5764	0.00
9.2	5361	0.00
9.5	4960	0.00

Supplemental Table 3: ESI MS Results for PurE Mutants		
	Observed Mass	Expected Mass
WT Enzyme	17,650.4	17,650.1
H45N	17,626.0	17,626.0
H45Q	17,640.0	17640.1
H45W	17,698.0	17,698.2

Supplemental Table 4. SV-AUC Results for WT and Mutant PurE Proteins

Protein	Predicted MW (Da)	Observed MW (Da)	RMSD of Fit of SV-AUC Data
WT	141,200	140,740	0.0046
H45N	141,010	146,430	0.0044
H45Q	141,120	149,940	0.0043
H45W	141,590	139,500	0.0045

Supplemental Table 5. Summary of the available PurE structures

PDB ID	organism	mutation	pH	monomers per asu	ligand *
1QCZ	*E. coli*	wt	8.0	1	none
1XMP	*B. anthracis*	wt	7.5	8	none
2FWA	*A. aceti*	H89N	7.0	2	none
2FWB	*A. aceti*	H89F	8.0	2	none
2FW7	*A. aceti*	H59N	8.0	2	none
2FW8	*A. aceti*	H89G	8.0	2	none
1Q4V	*T. maritima*	wt	5.6	1	sulfate
2FW9	*A. aceti*	H59F	8.0	2	sulfate/none
2FW1	*A. aceti*	wt	8.5	2	acetate A/acetate B
1U11	*A. aceti*	wt	5.4	2	citrate A/citrate B
2FW6	*A. aceti*	H59N	5.4	2	citrate/none
1D7A	*E. coli*	wt	8.0	8	AIRx (4)/none(4)
2FWI	*A. aceti*	H59D	7.0	2	AIR/none
2FWJ	*A. aceti*	wt	7.0	2	AIR/none
2FWP	*A. aceti*	H59N	5.4	2	isoCAIR/citrate
	E. coli	H45N	8.0	1	CAIR
	E. coli	H45Q	8.0	1	CAIR
2ATE	*E. coli*	wt	8.0	1	nitroAIR
	E. coli	H45Q	8.0	1	nitroAIR

*PurE octamers containing bound ligands and multiple monomers per asymmetric unit usually show the same ligand structure for fourfold related monomers and different ligand structures for twofold related monomers. The two different ligand structures corresponding to the latter case are separated by a slash.

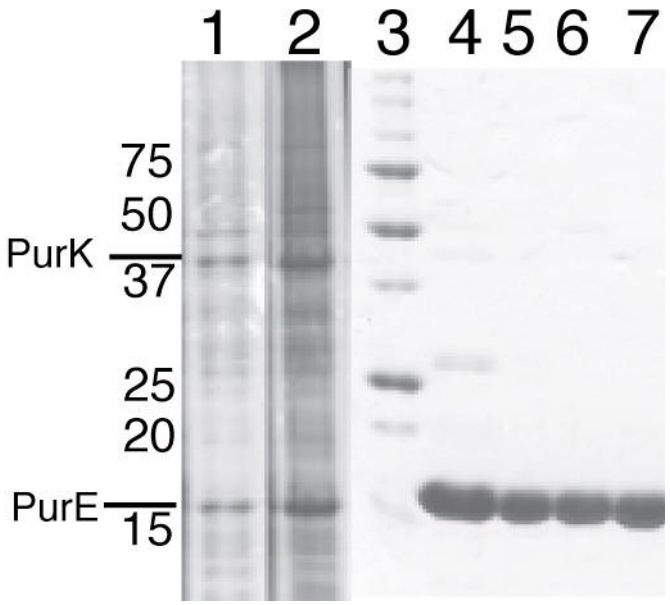

Supplemental Figure 1: 15% SDS-PAGE Gel of PurE Proteins. Lane 1: total cell lysate of wt PurE/PurK expression in PCO135 *E. coli* t = 0 h; 2: total cell lysate at t = 4 h after heat induction; 3: MW Markers; 4: wt PurE; 5: H45Q PurE; 6: H45W PurE; 7: H45N PurE. For lanes 4-7, 5 µg of protein was loaded.

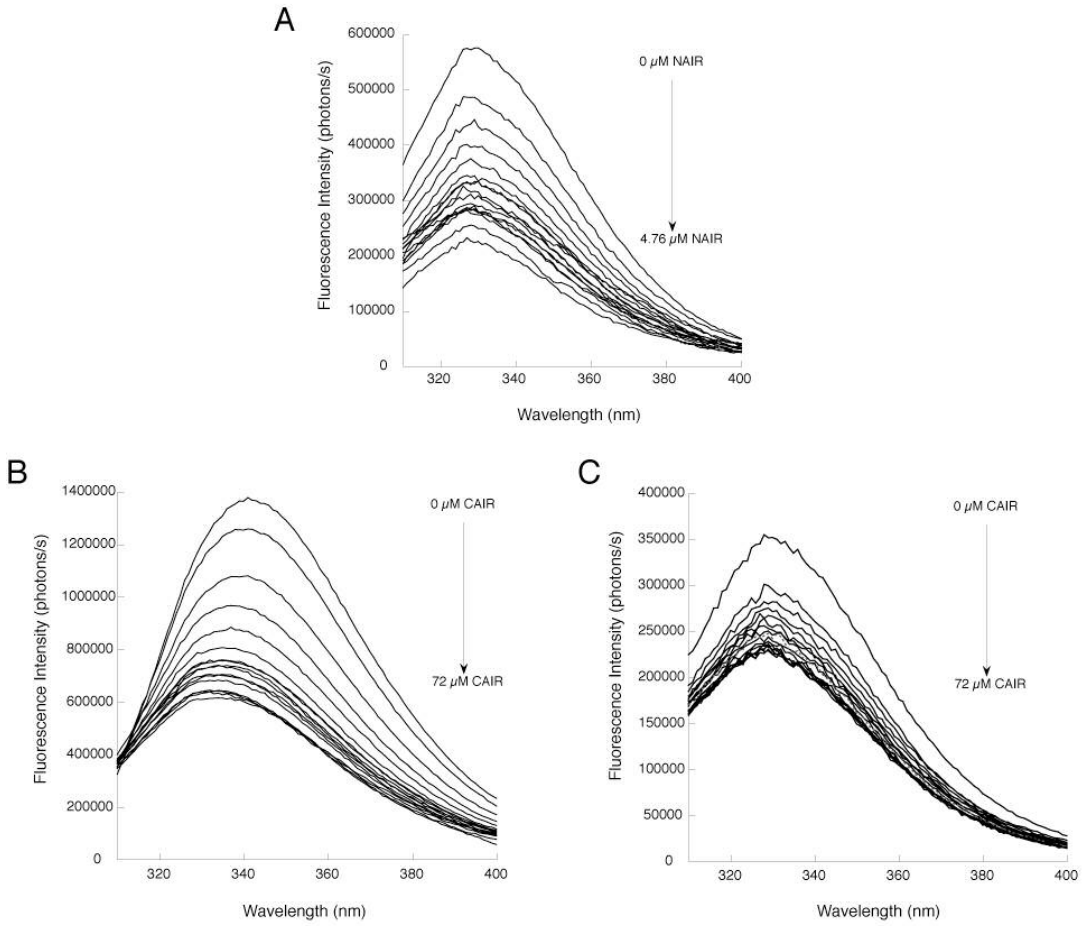

Supplemental Figure 2: Observed changes in fluorescence upon titration of PurE. (A) Titration of wt PurE with NO_2-AIR. (B) Titration of H45N PurE with CAIR. (C) Titration of H45Q PurE with CAIR. After background subtraction, fluorescence decreases at a λ_{max} of 335 nm for (A) and (C) and a decrease and blue shift from 345 → 335 nm (B) were observed.

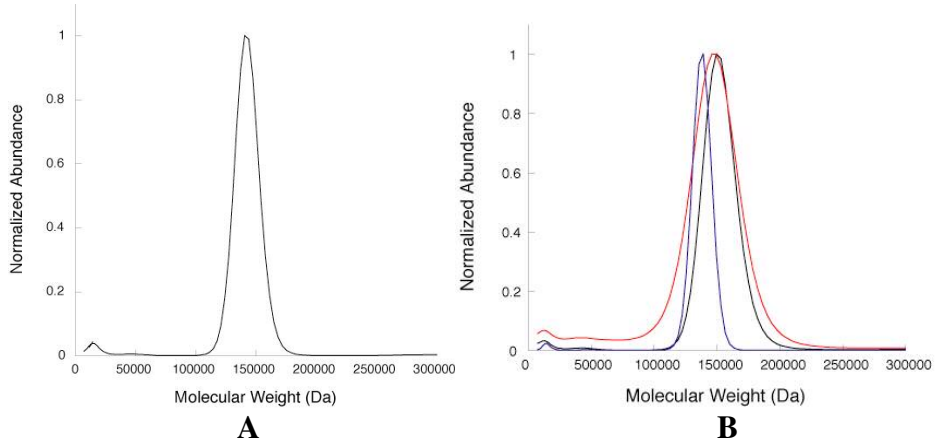

Supplemental Figure 3: Distribution of molecular weights obtained from SedFit analysis of SV-AUC data for PurE mutants. (A) wt PurE. (B) H45N (black), H45Q (red), and H45W (blue) PurE mutants.

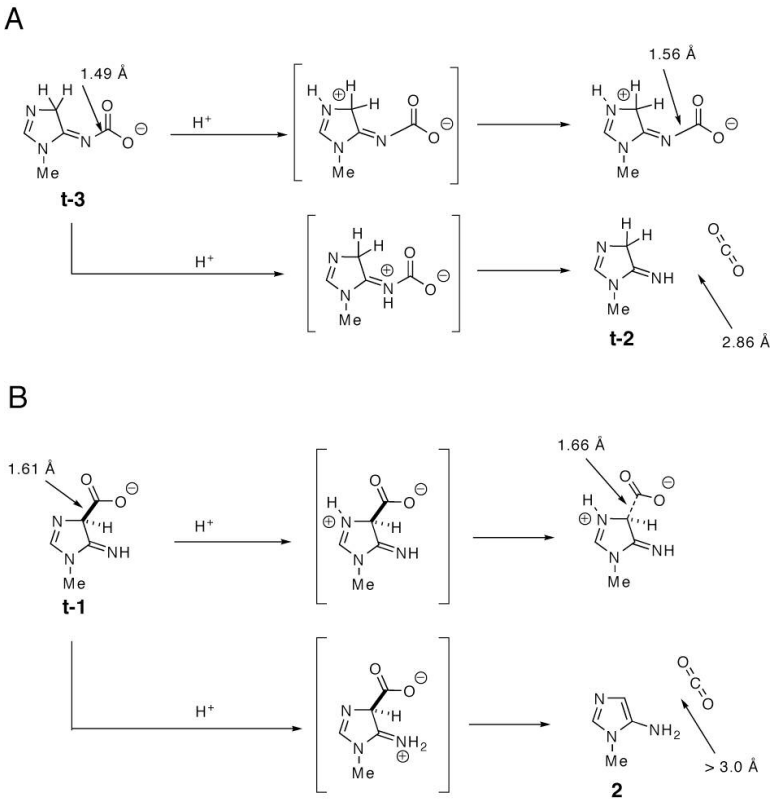

Supplemental Figure 4: Computational studies on the effects of protonation of compounds **t-3** and **t-1** on loss of CO_2 and bond lengths.

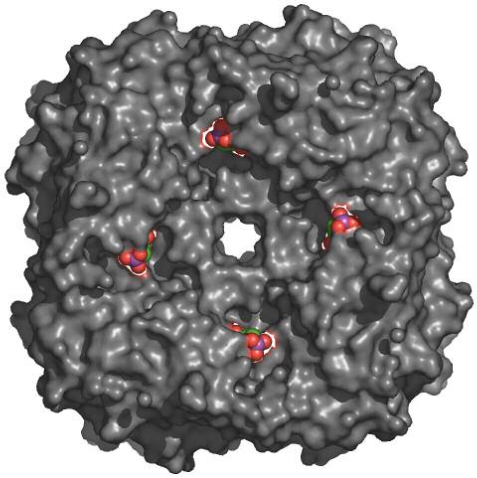

Supplemental Figure 5: Surface representation of the wt PurE octamer in grey. NO_2-AIR molecules on one face of the octamer are shown in spacefilling representation and colored using a CPK scheme. NO_2-AIR binds close to the surface. While the ribose-5'-phosphate moiety is exposed to the solvent, the aminoimidazole and nitro groups are buried.

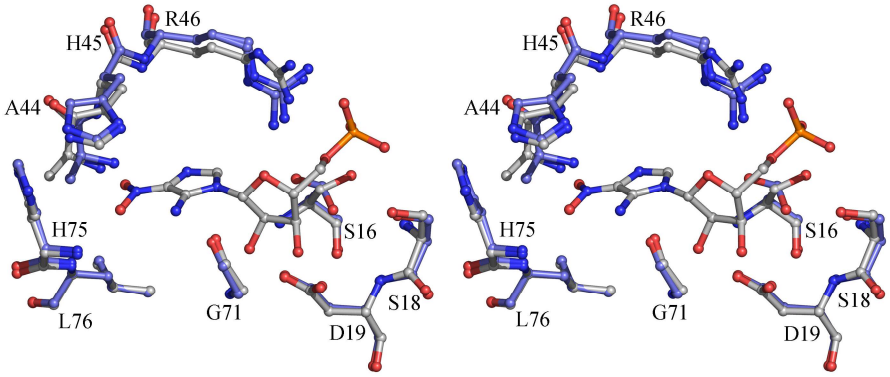

Supplemental Figure 6. Overlay of the active sites of apo wt EcPurE (blue) and the wt EcPurE NO_2-AIR co-crystal structure (grey). Conformational changes occurring upon ligand binding are limited to residues involved in binding the 5'-phosphate.

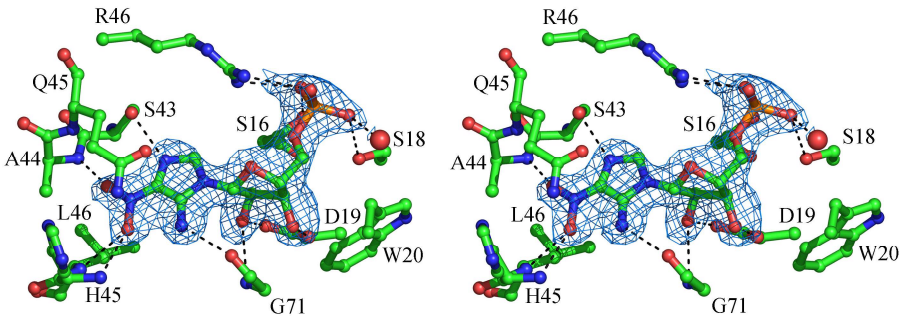

Supplemental Figure 7. Active site of EcPurE-H45Q-NO_2-AIR complex with fo-fc density (2σ) shown.

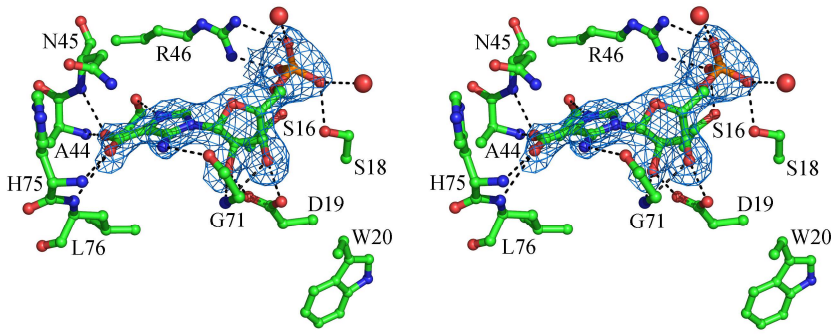

Supplemental Figure 8. Active site of EcPurE-H45N-CAIR complex with fo-fc density (2σ) shown.

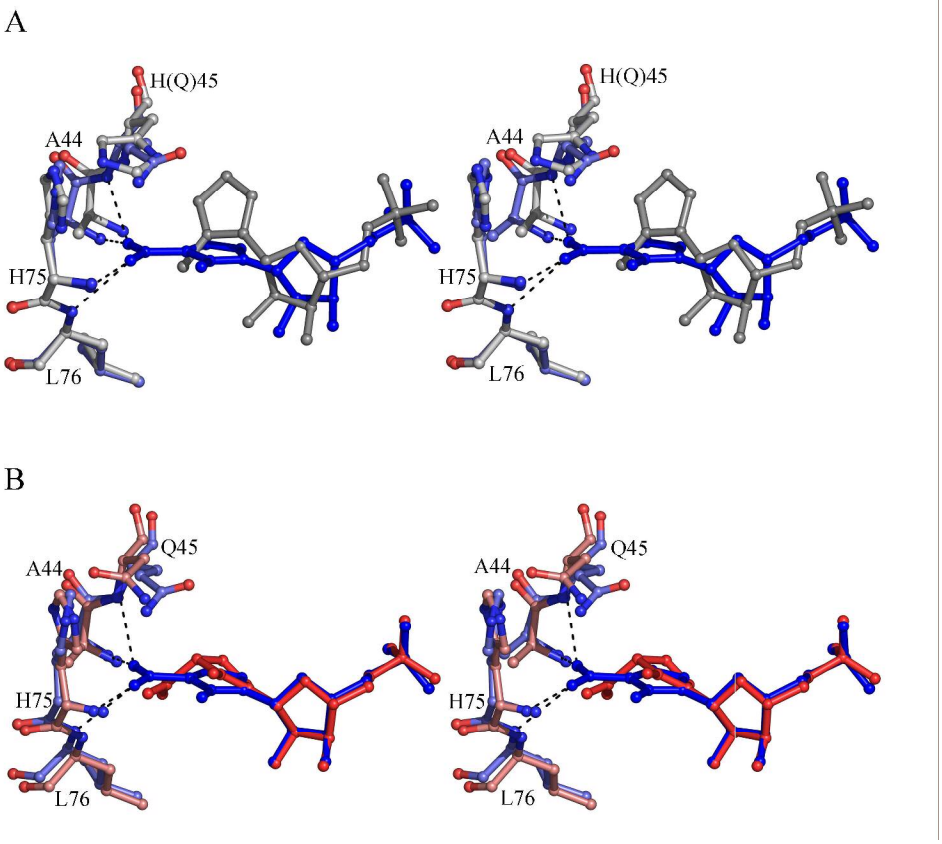

Supplemental Figure 9. A comparison of substrate binding conformations in PurE. (A) Superposition of H45Q EcPurE with CAIR (blue) and wt EcPurE-AIRx (grey). (B) Superposition of H45Q EcPurE with CAIR (blue) and isoCAIR from H59N AaPurE (red).

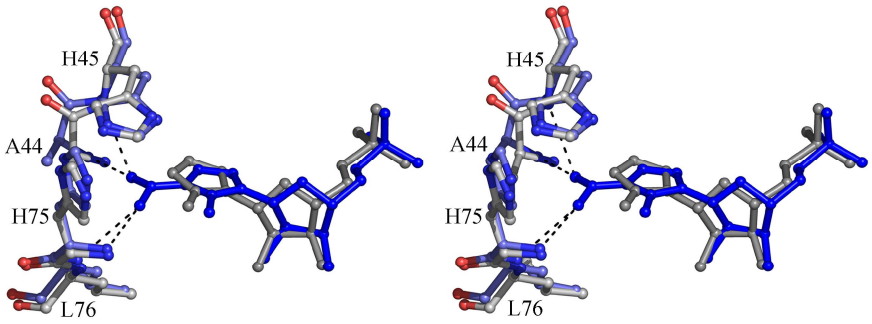

Supplemental Figure 10. Comparison of the NO_2-AIR/EcPurE (wt) with AIR/AaPurE (wt) complexes. EcPurE is in blue, AaPurE is in grey. Numbering is for EcPurE.